Structural Engineering and Mechanics, Vol. 31, No. 4 (2009) 371-382
DOI: http://dx.doi.org/10.12989/sem.2009.31.4.371

Behavior of high-strength fiber reinforced concrete plates under in-plane and transverse loads

Ramadoss, P.†

Department of Civil Engineering, Pondicheery Engineering College, Puducherry-605 014, India

Nagamani, K.‡

Structural Engineering Division, Civil Engineering Department, Anna University, Chennai-600 025, India

(Received May 7, 2007, Accepted February 1, 2009)

Abstract. The concrete plates are most widely used structural elements in the hulls of floating concrete structures such as concrete barges and pontoons, bridge decks, basement floors and liquid storage tanks. The study on the behavior of high-strength fiber reinforced concrete (HSFRC) plates was carried out to evaluate the performance of plates under in-plane and transverse loads. The plates were tested in simply supported along all the four edges and subjected to in-plane and traverse loads. In this experimental program, twenty four 150 mm diameter cylinders and twelve plate elements of size 600 × 600 × 30 mm were prepared and tested. Water-to-cementitious materials ratios of 0.3 and 0.4 with 10% and 15% silica fume replacements were used in the concrete mixes. The fiber volume fractions, V_f = 0%, 1% and 1.5% with an aspect ratio of 80 were used in this study. The HSFRC mixes had the concrete compressive strengths in the range of 52.5 to 70 MPa, flexural strengths ranging from 6.21 to 11.08 MPa and static modulus of elasticity ranging from 29.68 to 36.79 GPa. In this study, the behavior of HSFRC plate elements subjected to combined uniaxial in-plane and transverse loads was investigated.

Keywords: steel fiber reinforced concrete; silica fume; steel fibers; static mechanical properties; axial loads; plate elements; out-of-plane central deflection.

1. Introduction

The most promising materials used in construction today are the concrete fiber composites. Steel fiber reinforced concrete (SFRC) is increasingly used day by day as a structural material. Balaguru and Shah (1992), and ACI Committee 544 (ACI 544.4R-1989) have reported that the addition of steel fibers in concrete matrix improves all mechanical properties of concrete such as flexural strength, tensile strength, compressive strength, and impact strength, toughness and energy absorption capacity. Due to the inherent brittleness of HSC/HPC, it lowers its post-peak portion of the stress-strain diagram almost vanishes or descends steeply (ACI 363-92). This inverse relation between the strength and ductility is a serious drawback for the use of HSC/HPC and a compromise

† Ph.D., E-mail: dosspr@gmail.com
‡ Professor

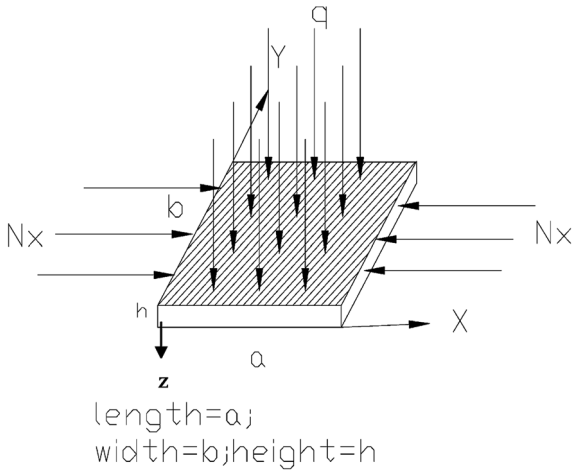

Fig. 1 Plate dimension, coordinate axes, and loading

to this drawback can be obtained by the addition of discontinuous short steel fibers of smaller diameter in to the concrete.

Concrete plates are used as structural elements in the hulls of floating concrete structures such as barges and pontoons, floating bridges and liquid storage tanks. These plate elements are subjected to combined compressive in-plane loads due to the longitudinal bending of structure, and transverse loads caused by hydrostatic pressure or deck loads. These plates resist loads in two way action and develop biaxial curvatures. Test results are available in the literature for reinforced concrete plates and steel plates supported along all the edges and subjected to in-plane loads or transverse loads (out-of-plane loads), and combined in-plane and lateral loads (Swartz *et al.* 1973, Aghayere and MacGregor 1990a, 1990b, Ghoneim and MacGregor 1994a, 1994b, Park and Kim 1999, Bambach and Rasmussen 2004, Roberts-Willmann 2004, Noh and Choi 2005, Malekzadev 2007, Bao *et al.* 1997), but for the writers' knowledge no published data are available for the steel fiber reinforced concrete plates subjected to lateral loads or in-plane loads or combined load situation.

An experimental program was carried out to investigate the behavior of HSFRC subjected to in-plane and transverse loads. This paper presents the results of tests on square steel fiber reinforced concrete plates subjected to combined loads or transverses load only. The experimental program consists of tests of twelve HSFRC square plates simply supported along all edges subjected to combined loads as shown in Fig. 1. The aspect ratio (a/b or L_x/L_y) of all the plates is 1 and length to thick ratio is maintained as 20. In each series, one plate element was tested under transverse load for the biaxial bending behavior alone and other two elements were tested under combined compressive in-plane and a uniform transverse loads. The applied in-plane load capacity of the plate cross section is taken as ($0.1f_c'$ bh) corresponding to the axial load capacity of the strip of plate considered as a short column. This paper describes the behavior of series of SFRC plates when loaded to failure under combined compressive in-plane and uniform transverse loads.

Research significance:

Most of the research carried out on plates under combined loads has been conducted on metal plates. Although concrete plates supported along all edges are used in the hulls of concrete barges and pontoons, floating bridges, basement floors, storage tanks and bridge decks, no such published

data available for steel fiber reinforced concrete composite plates subjected to combined in-plane and transverse loads. The tests and investigations reported in this paper partially fill this gap.

2. Test specimens

The test program was divided into four series (series A, B, C and D) of plates simply supported along four edges.

Series A consisted of three square specimens of size 600 × 600 × 30 mm. Specimens A1 & A2 tested under combined in-plane and uniform transverse loads and specimen A3 tested under uniform transverse load only.

Series B consisted of three square specimens of size 600 × 600 × 30 mm. Specimens B1 & B2 tested under combined in-plane and uniform transverse loads while the specimen B3 tested under uniform transverse load only.

Series C consisted of three square specimens of size 600 × 600 × 30 mm. Specimen C1 & C2 tested under combined in-plane and uniform transverse loads and specimen C3 tested under uniform transverse load only.

Series D consisted of three square specimens of side 600 × 600 × 30 mm. Specimen D2 & D3 tested under combined in-plane and uniform transverse loads while the specimen D1 tested under uniform transverse load only.

3. Materials and mixture proportions

Ordinary Portland cement-53 grade conforming to IS: 12269-1987 with a 28-day compressive strength of 54.5 MPa and condensed silica fume (in a powder form to achieve high-strength), contained 88.7% of SiO_2, having fineness by specific surface area of 23000 m^2/kg, a specific gravity of 2.25 were used in the ratio of 9:1 and 8.5:1.5 by weight of cementitious materials at each w/cm ratio of mixes.

Fine aggregate of locally available river sand passing through 4.75 mm IS sieve, conforming to grading zone-II of IS: 383-1978 was used. It has fineness modulus of 2.65, specific gravity of 2.63 and water absorption of 0.98% @ 24 hrs.

Coarse aggregate of crushed blue granite stones with 12.5 mm maximum size, conforming to IS: 383-1978 was used. The characteristics of coarse aggregate are: Specific gravity (SSD) = 2.70, Fineness modulus = 6.4, Dry rodded unit weight = 1600 kg/m^3 and Water absorption = 0.65% @ 24 hrs.

Superplasticizer of sulphonated naphthalene formaldehyde (SNF) condensate as HRWR admixture conforming to ASTM Type F (ASTM C494) and IS: 9103-1999 was used. It has a

Table 1 Crimped steel fiber characteristics

Geometry and properties	Value
Fiber diameter, d (mm)	0.45
Fiber length, l (mm)	36
Aspect ratio, l/d	80
Ultimate tensile strength, f_u (MPa)	910
Elastic modulus, E_f (GPa)	200

Table 2 Mixture proportions for HSFRC

Mix Designation	w/cm	Cement kg/m^3	Silica fume kg/m^3	Sand ratio (%)	Steel fiber V_f(%)	Super-plasticizer kg/m^3
FC1-0	0.4	394.2	43.8	38.8	0	7.66
FC1-1	0.4	394.2	43.8	38.8	1	7.66
FC1-1.5	0.4	394.2	43.8	38.8	1.5	7.66
FC1*-0	0.4	372.3	65.7	38.8	0	7.66
FC1*-1	0.4	372.3	65.7	38.8	1	7.66
FC1*-1.5	0.4	372.3	65.7	38.8	1.5	7.66
FC2-0	0.3	495	55	36.4	0	13.75
FC2-1	0.3	495	55	36.4	1	13.75
FC2-1.5	0.3	495	55	36.4	1.5	13.75
FC2*-0	0.3	467.5	82.5	36.4	0	13.75
FC2*-1	0.3	467.5	82.5	36.4	1	13.75
FC2*-1.5	0.3	467.5	82.5	36.4	1.5	13.75

In mix designations FC1 to FC2 and FC1* to FC2*, silica fume replacement is 10 percent and 15 percent respectively by weight of cementitious materials, after hyphen denotes fiber volume fraction in percent.
Water present in super plasticizer (SP) is excluded in calculating the water to cementitious materials ratio.
V_f(%) denotes steel fiber volume fraction in percent in total volume of concrete.
w/cm denotes water to cementitious materials ratio and cm = OPC + SF.

specific gravity of 1.20.

Fibers conforming to ASTM A820-01 have been used in this investigation, are crimped steel fibers (undulated). Properties of fibers are given in Table 1.

Mixtures were proportioned using guidelines and specifications given in ACI 211.4R-93, and recommended guidelines of ACI 544.3R-1993. Mixes that contained 10% and 15% silica fume as 1:1 partial replacement of cement. Mixture proportions used in this test program are summarized in Table 2. For each water-cementitious materials ratio, two fibrous concrete mixes were prepared with fiber volume fractions, V_f = 1.0 and 1.5 percent by volume of concrete (78 and 117.5 kg/m^3). Super-plasticizer with dosage of 1.75 and 2.25% by weight of cementitious materials has been used to maintain the adequate workability of plain (SF concrete) and fibrous concrete.

12 series of high-strength fiber reinforced concrete mixes with two w/cm ratios of 0.4 and 0.3 were used in this investigation. Concrete was mixed using a tilting type mixer and specimens were cast using steel moulds, compacted by table vibrator for external vibration. For each mix at least three 150 mm diameter cylinders and three 100 × 100 × 500 mm prisms were produced. 12 plate elements (size: 600 × 600 × 30 mm) were cast and produced. The aluminum channel section mould was used for casting the concrete plates. Specimens were demoulded 24 hours after casting and cured at 27 ± 2°C in water until the testing age of 28 days. For all the specimens same curing condition was maintained to avoid the variation of strength among the specimens.

4. Mechanical properties

4.1 Compressive strength

Compressive strength test were performed according to ASTM C 39-92 standards using 150 mm

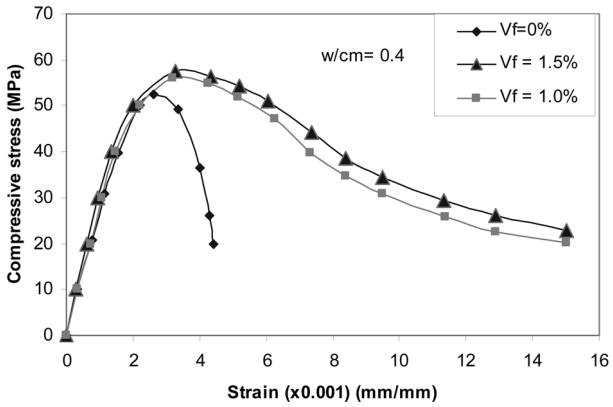

Fig. 2 Typical stress-strain curves for SF concrete and fibrous concrete and effect of fiber content on stress-strain curves

diameter cylinders loaded uniaxially. Before testing, the cylinders were capped with a hard plaster on the cast faces to ensure parallel loading faces of the test specimens and constant height for all cylinders. Three samples were used for computing the average strength.

4.2 Modulus of elasticity

According to ACI 318-92, modulus of elasticity (E_c) is defined as the slope of the line drawn from a stress of zero to $0.45f_c'$. The static modulus of elasticity was determined from the stress-strain curve of the fiber reinforced concrete as a result of test on cylinders for compression loading. Typical stress-strain curves for silica fume concrete (HSC) and steel fiber reinforced concrete (SFRC) are shown in Fig. 2.

4.3 Flexural strength

The flexural strength (Modulus of rupture) tests were conducted as per the specification of ASTM C 78-94 using 100 × 100 × 500 mm prisms under third- point loading on a simply supported span of 400 mm The tests were conducted in a 100 kN closed loop hydraulically operated Universal testing machine. Samples were tested at a deformation rate of 0.1 mm/min.

4.4 Ultrasonic pulse velocity

Ultrasonic pulse velocity (UPV) test was performed for the qualitative measurement of HSFRC mixes. The principle is that if the concrete is dense, then the wave will pass through the concrete quickly. Here the density can be checked with respect to the velocity of the pulse waves passing through each cylindrical concrete specimen. A suitable apparatus and a standard procedure are described in ASTM C 597. The variation in pulse velocity was marginal, indicating the uniformity in compaction of the concrete mixes. Visual observation of the surface of the specimens indicated the uniform distribution of fibers in the mixes.

Table 3 lists the compressive strength, flexural tensile strength, static modulus of elasticity, and ultrasonic pulse velocity for each plate specimen at 28-days of testing.

Table 3 Results of compressive and flexural strength, elastic modulus and pulse velocity of HSFRC

Mix designation	Specimen	RI	f'_{cf} (MPa)	f_{rf} (MPa)	E_c (GPa)	ν (from correlation of data)	UPV (m/s)
FC1-0	A1	0	52.56	6.21	29.68	0.19	4298
FC1-1	A2	2.58	56.01	7.73	30.92	0.20	4367
FC1-1.5	A3	3.88	57.42	8.19	31.78	0.21	4524
FC1*-0	B1	0	55.7	6.84	30.89	0.20	4318
FC1*-1	B2	2.58	60.21	8.64	32.75	0.22	4435
FC1*-1.5	B3	3.88	61.17	9.28	33.14	0.22	4559
FC2-0	C1	0	63.86	7.4	34.14	0.23	4516
FC2-1	C2	2.58	68.91	9.32	36.52	0.24	4667
FC2-1.5	C3	3.88	69.67	10.13	36.53	0.25	4790
FC2*-0	D1	0	64.28	8.16	34.39	0.23	4615
FC2*-1	D2	2.88	69.74	10.32	36.56	0.25.	4889
FC2*-1.5	D3	3.88	70.32	11.08	36.79	0.25	5004

RI = fiber reinforcing index.
f'_{cf} = cylinder compressive strength at 28 days; f_{rf} = flexural strength at 28 days.
E_c = secant modulus of elasticity; ν = Poisson's ratio; UPV = ultrasonic pulse velocity.

5. Test set-up

The test frame fabricated to resist the loading of the SFRC plates and used in this study is shown in Fig. 3. The frame was designed to carry the maximum transverse load of 100 kN. The test frame

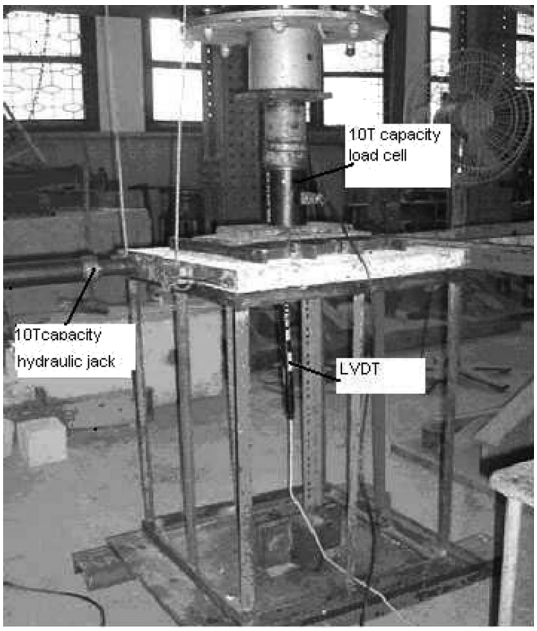

Fig. 3 Overall view of test frame set-up during test of specimen

consisted of a supporting frame for plates, lateral loading system, and independent loading unit for applying the in-plane load. The plate specimen was supported on the 4-ISA 30 × 30 × 6 mm, which are welded on the eight legs of 28 mm RTS rods, 4 legs on 4 corners and remaining 4 legs of one each in between the two corner legs to form the stable test frame. The bottom of eight legs is connected on the four angle sections. For applying in-plane loads to the specimens, 100 kN capacity hydraulic jack mounted with the M.S. channels, was used. The channels are firmly fixed by bolted connections on the sides of the loading frame of capacity 100 T (1000 kN). The in-plane load was applied in the x-direction using 10 T (100 kN) capacity loading jack. The transverse load was read using a 100 kN capacity load cell and the load was applied through a 600 kN (60 T) capacity loading jack which was attached to a 100 T capacity loading frame. The loading frame was firmly fixed on the testing floor.

Instrumentation

Displacement was recorded electronically using a linear variable displacement transducer (LVDT) with least count of 0.01 mm. LVDT was placed at mid span of the bottom of the plate element to measure the central surface deflection. The working conditions of transducers were checked by applying minimum load, and then dropped to zero. Syscon load cell of 10 T capacity, connected to 3 channel load indicator was used to measure the lateral load with least count of 10 kg.

6. Test procedure

The plate being tested was first pre-loaded to approximately 100 kg load. This allowed the structural element to settle and all the instrumentation was checked to ensure that it was working properly. The plate was then unloaded and all gauges were zeroed. For specimen A3, the transverse load was applied simultaneously from zero to the maximum load until failure of the specimen. The center deflection readings of the specimen at different loading intervals were noted. The failure of the specimen was considered as the cracking behavior of the concrete plate. For the specimens A1 and A2, the in-plane loads were applied incrementally first to its selected value and thereafter, the in-plane load was allowed until failure (kept constant) while transverse loads were applied monotonically and incrementally from zero to maximum value and then allowed to drop-off steadily up to the failure of the specimens. At each load increment, the cracks were marked and deflection readings were taken. For all other series (i.e., series B, C, and D), the same procedure as detailed above was followed.

7. Test results and discussion

The mechanical properties of silica fume concrete reinforced with crimped steel fibers are presented in Table 3. Table 4 shows the properties of each specimen as well as the maximum transverse load per unit area, and the uniform in-plane load per unit width applied in the x-direction. The variation of in-plane load during the application of transverse was less than 1 percent. The total transverse load calculated in kN was applied through load cell placed over the load distribution assembly, which then distributed uniformly on the specimen. The in-plane load is given in kN/m as the hydraulic load divided by 0.6 m.

Table 4 Summary of experimental program and test results

Specimen	$L_x = L_y$ (mm)	L_y/L_x	L_x/h	f'_{cf} (MPa)	Applied Nx (kN/m)	$N_x/f'_{cf} \cdot h$	q (kN/m^2)
A1	600	1	20	52.56	100	0.063	92.22
A2	600	1	20	56.01	100	0.060	125.27
A3	600	1	20	57.42	0	0	93.06
B1	600	1	20	55.7	100	0.060	106.11
B2	600	1	20	60.21	100	0.055	129.44
B3	600	1	20	61.17	0	0	95.83
C1	600	1	20	63.86	100	0.052	115.28
C2	600	1	20	68.91	100	0.048	133.33
C3	600	1	20	69.67	0	0	99.44
D1	600	1	20	64.28	0	0	65.83
D2	600	1	20	69.74	100	0.048	142.78
D3	600	1	20	70.32	100	0.047	159.86

$L_x = L_y$ = 600 mm; h = thickness of plate = 30 mm; aspect ratio = Ly/Lx =1
N_x = in-plane load per unit width in x-direction (kN/m); q = transverse load per unit area (kN/m^2)

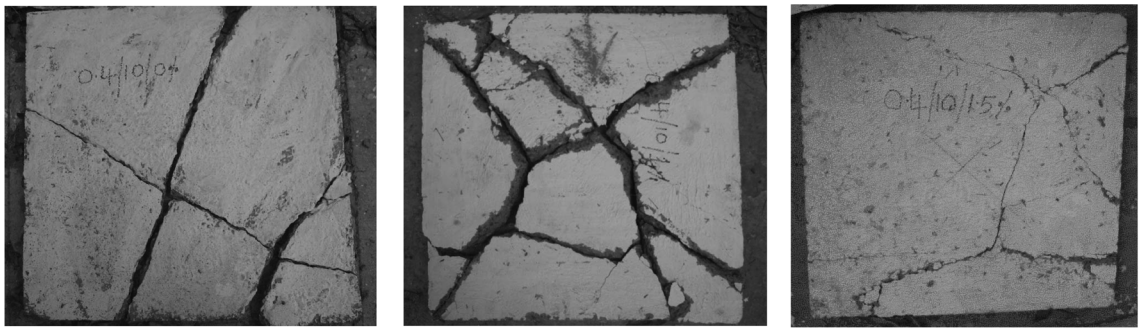

(a) (b) (c)

Fig. 4 (a) Fracture pattern of test specimen after ultimate failure (Plate A1), (b) Fracture pattern of test specimen after ultimate failure (Plate A2), (c) Fracture pattern of test specimen after ultimate failure (Plate A3)

Specimens A1 and A2 were tested for combined compressive in-plane and transverse loads, while the specimen A3 was subjected to transverse load only to give indication of the reduction in capacity for specimens within the same series, for comparing the crack patterns. In the specimen A1, fracture occurred at a center deflection of 4.63 mm with transverse load of 92.22 kN/m^2, and failure was sudden and explosive. Further concrete crushing lines were observed and cracks were more prevalent in x-direction. The pattern of cracking and crushing are shown in Figs. 4(a), (b) and (c). In the specimen A2, cracks were first observed at the bottom of the specimen in the direction of in-plane load (x-direction) at a transverse load of 125.27 kN/m^2. The center deflection at maximum transverse load was 11.32 mm. Final failure occurred at a center deflection of 14.53 mm.

Cracks were first observed for specimen A3 on the flexural tension (bottom) face as it fails by

attaining the ultimate flexural tensile strength, at a transverse load of 93.06 kN/m^2 and center deflection at this load was 5.19 mm. Yield lines were formed on the tension face of the specimen at maximum load. Cracks were observed along the diagonal on the bottom face near the corners (Figs. 4(a), (b) and (c)). In addition, cracks were developed perpendicular to the diagonal on the top surface near the corners. These corners resulted from the corners being held down. This indicates the torsion cracks on the edge of the plate caused due to twisting moment occurred near the corners. At the ultimate load all the specimens that were tested under combined loads was in a state of axial compression at the middle of the plane, since the principal moments were both positive. For all other series except series D (i.e., series B, and C), the same combination of loading should be applied and tested and the observations should be noted. In series D, specimen D1was considered for transverse load only and other specimens (i.e., D2 and D3) were considered for combined loads.

Load-deflection response

The transverse load verses out-of-plane deflection relationships for plate specimens except plate D1, tested under lateral loads only exhibited similar features. Figs. 5-8 show the transverse load verses out-of-plane deflection (P-Δ) at the center of the plate specimen. The SFRC specimens exhibited essentially a linear P-Δ response well beyond the load while the flexural cracks were first observed during the test. Each diagram is essentially a straight line up to the start of cracking. Beyond cracking, a rapid change of slope in the load deflection curve was observed. On further loading yielding of fibers started in one or more regions and spread through the areas still elastic. This continued till the yield line mechanism developed. A small out-of-plane deflection occurred in several specimens during the application of the in-plane loads. This deflection ranged from 0-2% of the transverse load. Zero deflection corresponding to the un-cracked plate in the horizontal position supporting its own weight.

The level of the in-plane load ($Nx/f_c'.h$) for all the specimens was moderate, in the sense that there are no possibility of collapse under in-plane load alone. Table 4 gives the ratio of the applied in-plane load per unit width to the uniaxial strength of concrete multiplied by the panel thickness for all of the specimens. The test results and predicted yield capacity for specimens tested under transverse (lateral) load only are given Table 5.

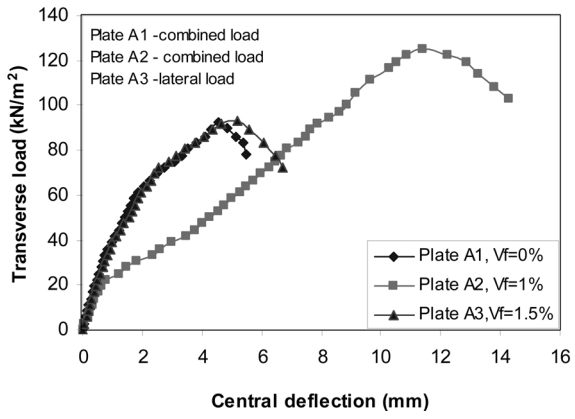

Fig. 5 Transverse (lateral) load versus Out-of-plane central deflection for plate specimens (Series A)

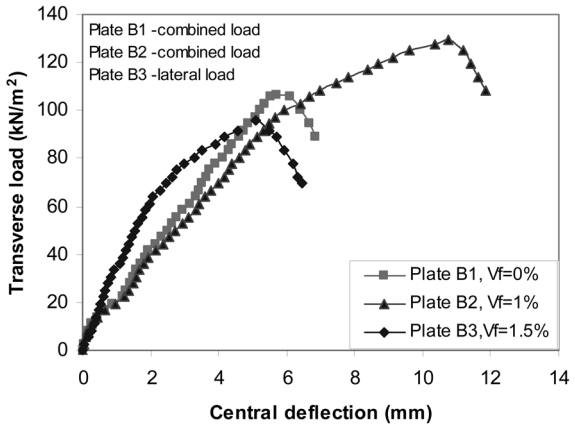

Fig. 6 Transverse load versus Out-of-plane central deflection for plate specimens (Series B)

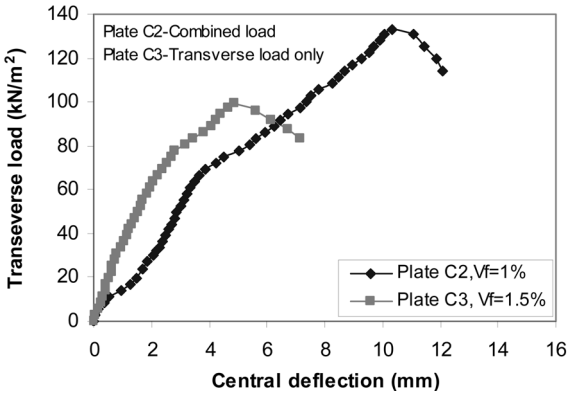

Fig. 7 Transverse load versus Out-of-plane central deflection for plate specimens (Series C)

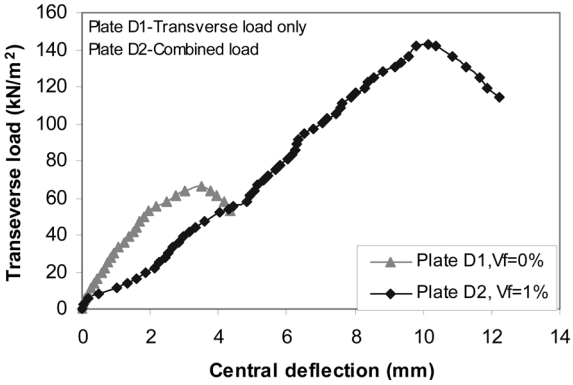

Fig. 8 Transverse load versus Out-of-plane central deflection for plate specimens (Series D)

Table 5 Test results and predicted theoretical (yield) capacity for specimens tested only under lateral loads

Specimen	L_y/L_x	L_x/h	q_{test} kN/m^2	q_{theo} kN/m^2	$q_{test}/q_{theo.}$
A3	1	20	93.06	60.94	1.527
B3	1	20	95.83	69.05	1.388
C3	1	20	99.44	73.95	1.345
D1	1	20	65.83	59.56	1.105

q_{theo} was obtained using yield-line analysis.
q_{test} corresponds to experimental values.

8. Conclusions

Based on the results of this investigation, the following conclusions are drawn:

1. Plate specimens tested under transverse loads only carried loads higher than those predicted by the yield-line analysis. This is partly attributed to the increased flexural toughness, strain softening and improved fiber bond resistance of the fibrous concrete.
2. Specimens made of fibrous concrete, tested under combined compressive in-plane and transverse loads fail by ductile mode of failure by debonding of fibers from the concrete. The mode of failure of the plain concrete specimens was a brittle failure (concrete crushing).
3. The failure pattern of the specimens tested under combined in-plane and transverse loads showed the propagation of yield line is toward the direction of the in-plane load approaching near the corners. In addition, cracks developed perpendicular to diagonal on the surface near the corners. This indicates the torsion cracks on the edges of the plate caused due to the twisting moment occurred near the corners.
4. The loading sequence is a significant factor in determining the ultimate strength of plates subjected to combined loads. Proportional loading or prior application of in-plane load resulted essentially in the same lateral load-deflection response and the same ultimate strength.
5. For the two sequence considered, the loading sequence had a very minor effect on the load capacity of the plate.

Acknowledgements

The authors would like to thank the Structural Engineering Division of Anna University, India for extending the facilities for the above research work.

References

ACI Committee 211 (1999), Guide for Selecting Proportions for High Strength Concrete with Portland Cement and Fly Ash, ACI 211.4R-93, ACI Manual of Concrete Practice.

ACI Committee 363 (1997), State-of-the-art Report on High-strength Reinforced Concrete, ACI 363-92, American Concrete Institute, Detroit.

ACI Committee 544 (2006), Guide for Specifying, Mixing, Placing and Finishing Steel Fiber Reinforced Concrete, ACI 544.3R-95, American Concrete Institute, Detroit.

ACI Committee 544-1989, Design Considerations for Steel Fiber Reinforced Concrete, ACI 544.4R-89, American Concrete Institute, Detroit.

Aghayere, A.O. and MacGregor, J.G. (1990a), "Test of reinforced concrete plates under in-plane and traverse loads", *ACI Struct. J.*, **87**(6), 615-622.

Aghayere, A.O. and MacGregor, J.G. (1990b), "Analysis of concrete plates under combined in-plane and tranverse loads", *ACI Struct. J.*, **87**(5), 539-547.

Balaguru, N. and Shah, S.P. (1992), Fiber Reinforced Concrete Composites, McGraw Hill International edition, New York.

Bambach, M.R. and Rasmussen, K.J.R. (2004) "Test of unstiffened plate elements under combined compression and bending", *J. Struct. Eng.*, **130**(10), 1602-1610.

Bao, G., Jiang, W. and Roberts, J.C. (1997), "Analytical and finite element solutions for bending and buckling of orthotropic plates", *Int. J. Solids Struct.*, **34**(14), 1797-1832.

Ghoneim, M.G. and MacGregor, J.G. (1994a), "Tests of reinforced concrete plates under combined inplane and lateral loads", *ACI Struct. J.*, **91**(1), 19-30.

Ghoneim, M.G. and MacGregor, J.G. (1994b), "Behavior of reinforced concrete plates under combined inplane and lateral loads", *ACI Struct. J.*, **91**(2), 188-197.

Malekzadeh, P. (2007), "A DQ nonlinear bending analysis of skew composite thin plates", *Struct. Eng. Mech.* **25**(2), 161-180.

Noh, H.C. and Choi, C.K. (2005), "Added effect of uncertain geometrical parameter on the response of variability of Mindlin plate", *Struct. Eng. Mech.*, **20**(4), 477-493.

Park, H. and Kim, E.H. (1999), "R.C. flat plates under combined in-plane and out-of plane loads", *J. Struct. Eng.*, ASCE, **125**(10), 1138-1142.

Ramadoss, P. and Nagamani, K. (2006), "Investigations on the tensile strength of high-performance fiber reinforced concrete using statistical methods", *Comput. Concrete.*, **3**(6), 389-400.

Ramadoss, P. and Nagamani, K. (2007), "Behavior of high-performance fiber reinforced concrete plates", Proceedings of International Conference on Recent Developments in Structural Engineering, RDSE-2007, MIT, Manipal, India, Aug./Sept.

Roberts-Willmann, C.L., Guirola, M. and Easterling, W.S. (2004), "Stength and performance of fiber-reinforced concrete composites slabs", *J. Struct. Eng.*, **130**(3), 520-528.

Swartz, S.E., Roseebraugh, V.H. and Berman, M.Y. (1973), "Buckling tests on rectangular concrete panels", *ACI J.*, 33-39.

Notation

HSFRC : High-strength fiber reinforced concrete.
q : Intensity of continuously distributed load, kN/m^2.
N_x : Normal force per unit length of section in x-direction, kN/m.
L_x or a : Length of plate in x-direction.
L_y or b : Length of plate in y-direction.
h : Thickness of plate element, mm
f'_{cf} : Compressive strength of HSFRC at 28 days, MPa.
f_{tf} : Flexural tensile strength of HSFRC at 28 days, MPa.
E_c : Static elastic (secant) modulus of HSFRC at 28 days, GPa
UPV : Ultrasonic pulse velocity of HSFRC at 28 days, m/sec.